

## X-ray magnetic circular dichroism at the Gd $L_{2,3}$ absorption edges in GdN layers: The influence of lattice expansion

F. Leuenberger,<sup>1</sup> A. Parge,<sup>1,2</sup> W. Felsch,<sup>1,\*</sup> F. Baudelet,<sup>3</sup> C. Giorgetti,<sup>4</sup> E. Dartyge,<sup>5</sup> and F. Wilhelm<sup>6</sup>

<sup>1</sup>*I. Physikalisches Institut, Universität Göttingen, Friedrich-Hund-Platz 1, D-37077 Göttingen, Germany*

<sup>2</sup>*IV. Physikalisches Institut, Universität Göttingen, Friedrich-Hund-Platz 1, D-37077 Göttingen, Germany*

<sup>3</sup>*Synchrotron SOLEIL, L'Orme des Merisiers, Saint-Aubin, B.P. 48, 91192 Gif-sur-Yvette Cedex, France*

<sup>4</sup>*École Polytechnique, LSI, 91128 Palaiseau Cedex, France*

<sup>5</sup>*Laboratoire pour l'Utilisation du Rayonnement Electromagnétique, Bâtiment 209 D, Université Paris-Sud, 91405 Orsay, France*

<sup>6</sup>*European Synchrotron Radiation Facility, B.P. 220, 38043 Grenoble Cedex, France*

(Received 3 March 2006; published 16 June 2006)

We have measured core-level x-ray-absorption spectra and x-ray magnetic circular dichroism (XMCD) at the Gd- $L_{2,3}$  edges to characterize the low-lying Gd- $5d$  derived conduction-band states in thin films of the  $4f$  ferromagnet GdN with a unit-cell volume 8.6% above that of bulklike layers. The nonequilibrium structure is obtained by  $N^+$  plasma-assisted reactive sputter deposition at room temperature. The Curie temperature  $T_C$ , a key quantity for magnetism, amounts to only half the bulk value of  $\sim 60$  K indicating a significant reduction of the effective exchange interaction between the  $4f$  states. An intricate observation is that the ratio of the dichroic signal amplitudes in the lattice-expanded layers,  $|L_3/L_2|$ , is up to three times higher than the value expected from the degeneracy of the  $2p_{3/2}$  and  $2p_{1/2}$  core states, which is observed for the bulklike layers. This is mainly due to a reduced  $L_2$  XMCD amplitude. We suggest that the effect may be related to the different weight the crystal-field split Gd- $5d$  final states ( $t_{2g}$  and  $e_g$ ) have in the absorption process at the  $L_2$  and  $L_3$  edges, and to the special electronic band structure of this strongly correlated material and its modification upon lattice expansion. This hypothesis is supported by the observation that the  $L_2$  absorption edge is shifted to lower energies upon ferromagnetic ordering while the  $L_3$ -edge position remains inert.

DOI: [10.1103/PhysRevB.73.214430](https://doi.org/10.1103/PhysRevB.73.214430)

PACS number(s): 75.50.Pp, 78.70.Dm, 87.64.Ni, 71.30.+h

### I. INTRODUCTION

The rare-earth (RE) compound GdN is a system with a strongly correlated electron structure and a low concentration of free charge carriers. The crystal structure is rocksalt (fcc). In spite of a considerable experimental and theoretical activity devoted to its fundamental properties for more than thirty years knowledge of the electronic and magnetic ground-state configuration is darkened by a number of conflicting observations. On the experimental side, the early discrepancies concerning magnetic order (ferromagnetic<sup>1-3</sup> or antiferromagnetic<sup>4,5</sup>) may be related to different degrees of sample perfection. In fact, due to the high melting point the synthesis of stoichiometric and uncontaminated GdN is difficult to achieve. The extreme sensitivity of the magnetic structure to deviations from stoichiometry, impurities, and lattice defects, which are manifest, for example, in the carrier concentration level and lattice spacing, was recognized very early by Wachter and Kaldis.<sup>4</sup> Li *et al.*<sup>6</sup> provided convincing experimental evidence that stoichiometric GdN is a ferromagnet with a Curie temperature  $T_C$  around 60 K and a magnetic saturation moment near  $7\mu_B/\text{Gd}$  ion consistent with the  $^8S_{7/2}$  half filled  $4f$ -shell configuration of  $\text{Gd}^{3+}$ . Recently Aerts *et al.*<sup>7</sup> predicted, on the basis of an *ab initio* electronic-structure calculation using the self-interaction corrected local-spin-density approximation (SIC-LSDA) to density-functional theory, a half metallic ground state for ferromag-

netic GdN with complete spin polarization of the itinerant band electrons, i.e., with only majority-spin electrons of essentially Gd ( $s, d$ ) and N  $p$ -like symmetry at the Fermi energy  $E_F$  and a small ( $\sim 0.9$  eV) indirect band gap for the minority spin channel. The density of electron states at  $E_F$  is expected to be very low. Yet, the half metallicity, suspected already in previous work,<sup>8,9</sup> has to be verified. If so, the compound will have a strong potential in spintronics applications. The ordered magnetism of GdN originates from the large local spin magnetic moments of the half filled Gd  $4f$  shell coupled by indirect exchange interactions. Exchange and hybridization induce spin splitting of the conduction-band states. As a result, the itinerant Gd- $5d$ - and N- $2p$ -derived band electrons carry small magnetic moments that are expected to oppose each other and to nearly cancel.<sup>7,9</sup>

In a recent publication<sup>10</sup> we report on the magnetic and transport properties of high-quality thin films of GdN prepared by reactive ion-beam sputtering. They show good stoichiometry, the lattice parameter, Curie temperature  $T_C$ , and saturation magnetization of the bulk material. The electrical conductivity is thermally activated down to the onset of ferromagnetic ordering where there is evidence of a transition to metallic behavior. The low value of the carrier activation energy ( $\sim 10$  meV) suggests highly degenerate  $n$ -type semiconducting behavior above  $T_C$ , possibly due to nitrogen vacancies acting as shallow donors.<sup>10</sup>

The transition to metallic conduction can be tuned by an external magnetic field, as is reflected by a giant negative magnetoresistance.

The present work is an extension of the previous study. Recently, Duan *et al.*<sup>11</sup> have shown by a first-principles calculation (LSDA+U approach) that the electronic structure and magnetic interactions in GdN depend sensitively on the interatomic distances which may vary, for example, due to external pressure or internal strain. This may not be surprising in view of previous experimental observations for this material<sup>4</sup> and theoretical results obtained for isovalent EuN.<sup>12,13</sup> We have grown GdN layers with an increased lattice parameter (named “lattice-expanded” hereafter), which permits us to study aspects of the magnetic properties of this compound in an out-of-equilibrium situation. Concerning the macroscopic properties, we find that the Curie temperature is significantly reduced in this state, pointing to a reduced exchange interaction as predicted.<sup>11</sup> To study the microscopic properties, core level x-ray-absorption (XA) spectroscopy and measurements of x-ray circular magnetic dichroism (XMCD) were employed. These techniques provide element and electronic-shell specific information on the electronic and magnetic properties of the material on a local level. We focus on the XA and XMCD spectra measured at the  $L_{2,3}(2p)$  photoabsorption edges of Gd to characterize the properties of the  $5d$ -derived band states in the “nonequilibrium” GdN layers. These states play a key role for the electronic and magnetic properties of the compound<sup>7,9,11</sup> and can be expected to sensitively mirror deviations from bulk equilibrium behavior. The XA and XMCD techniques were previously applied to the GdN layers with bulklike macroscopic properties<sup>10</sup> to study (i) the magnetic polarization of the Gd- $4f$  states and (ii) the N- $p$  character of the low-lying unoccupied electronic conduction-band states. As expected the spontaneous  $4f$  magnetic moment is close to  $7\mu_B/\text{Gd}$  ion; its temperature dependence mirrors the behavior of the macroscopic magnetization. The N- $2p$  states carry an ordered orbital magnetic moment in the ferromagnetic phase, supposed to be induced by hybridization with the Gd- $5d$  states.<sup>10</sup> XA and XMCD spectra involving transitions to the Gd- $5d$  states were not measured on the bulklike “equilibrium” GdN layers in the previous studies. Here, it was the main issue to probe the  $5d$  states, mainly on the lattice-expanded layers but also on a layer with bulklike properties as a reference. The XMCD technique was also used to measure the Gd- $4f$  magnetic moments in the lattice-expanded GdN layers. An unresolved problem well known in the RE community is that the theoretical understanding of the RE- $L_{2,3}$  XMCD spectra probing the  $5d$  states is limited owing to the exchange interaction between the  $5d$  and  $4f$  states.<sup>14–17</sup> A different aspect we find for the GdN layers somewhat unexpectedly is that an enhancement of the lattice parameter leads to a pronounced deviation of the ratio of the XMCD amplitudes at the Gd- $L_3$  and  $L_2$  absorption edges from the statistical value that is imposed by the degeneracy of the  $2p_{3/2}$  and  $2p_{1/2}$  core states and observed in the GdN layers with the equilibrium lattice parameter.

## II. EXPERIMENT AND BASIC SAMPLE CHARACTERISTICS

### A. Layer growth, structure, and macroscopic magnetic properties

Individual GdN layers (thickness up to 2000 Å) were grown by N<sup>+</sup> plasma-assisted reactive ion-beam sputtering of gadolinium with argon in an ultrahigh vacuum chamber (base pressure  $<5 \times 10^{-10}$  mbar). For details, the reader is referred to our previous publication.<sup>10</sup> During growth the background partial pressure of nitrogen was near  $2 \times 10^{-5}$  mbar, that of unwanted reactive gases (O<sub>2</sub>, CO) below  $10^{-10}$  mbar. Si(100) wafers served as substrates, essentially for basic characterization by x-ray diffraction, macroscopic magnetometry, x-ray photoelectron spectroscopy (XPS), and resonant nuclear reaction analysis (RNRA). Kapton- and Mylar-foil substrates (thickness 12 and 1.5 μm, respectively) were used for most of the XA and XMCD experiments to permit measurements in transmission mode. Cr or W buffer layers (40 Å) warranted identical growth conditions for the GdN layers, Cr or Al caps (50 Å) protected them against oxidation upon exposure to air. While the Kapton and Mylar substrates were held at room temperature during layer deposition the temperature  $T_S$  of the Si substrates was varied between room temperature and 450 °C, the optimal temperature for growing high-quality GdN layers with bulklike properties.<sup>10</sup>

Reducing  $T_S$  to room temperature has a significant influence on the growth of the layers: it enhances the lattice parameter significantly to above the bulk equilibrium value. X-ray diffraction in  $\Theta/2\Theta$  geometry revealed polycrystalline growth in the NaCl structure in each case, without foreign phases. XPS spectra proved the absence of oxygen impurities. Deposition at  $T_S=450$  °C leads to a lattice parameter of 1.5% above that of the bulk material and an average grain extension along the film normal of  $\sim 100$  Å. These films have bulklike properties<sup>10</sup> in spite of the small deviation from the equilibrium lattice parameter. The films grown at room temperature show a lattice parameter 4.4% above the bulk equilibrium value and a grain size near 50 Å, i.e., the latter films have an 8.6% larger unit-cell volume than the former ones. We note that this is observed for layer thicknesses as large as 2000 Å, irrespective of the substrates (Si or Kapton). As for the bulklike layers, deviations from the stoichiometry could not be detected for the films grown at room temperature; XPS using the Gd  $4d$  and N  $1s$  emission intensities and RNRA based on the process  $^{15}\text{N}(p, \gamma\alpha)\text{C}^{12}$  revealed that deviations from the one-to-one composition ratio of GdN are at most a few percent. Hence the observed lattice expansion cannot be the result of a significant nitrogen deficiency. According to superconducting quantum interference device magnetometry all GdN layers are good ferromagnets. Irrespective of  $T_S$ , their spontaneous magnetization is near the bulk value of  $\sim 7\mu_B/\text{Gd}$  ion at 4 K. However, the Curie temperature  $T_C$  is significantly diminished by the reduction of  $T_S$ : it lies near 30 K for GdN deposited at room temperature as compared to the bulk value of  $\sim 60$  K found for the layers deposited at  $T_S=450^\circ$ .<sup>10</sup> Hence the expansion of the GdN lattice leads to a sensible reduction of the effec-

tive exchange interaction. All layers are magnetically soft, with essentially the same shape of the magnetization curves  $M(H)$  at temperatures  $T \ll T_C$ . Finally we note that for each GdN layer the XPS spectrum in the valence-band region shows the same energy position of the  $\text{Gd}^{3+} 4f^6$  final-state multiplet near 8 eV below the Fermi level, i.e., the position of the occupied  $f$  states in the electron band structure of GdN is insensitive to the lattice expansion resulting from the variation of  $T_S$ .

### B. Measurement of x-ray absorption and magnetic circular dichroism

The XA spectra were acquired by means of different spectrometers. In the center of interest of this study are the  $L_{2,3}$  absorption edges of Gd, dominated by the electric-dipole-allowed  $2p \rightarrow 5d$  resonant transitions at photon energies in the hard x-ray range ( $\sim 7.2$ – $8.0$  keV). They were acquired at the energy-dispersive beamline D11 of the DCI storage ring at the French synchrotron facility LURE in Orsay (lattice-expanded GdN layers) and at the beamline ID12A of the European Synchrotron Radiation Facility (ESRF) in Grenoble, France (bulklike layer). The dispersive beamline D11 uses the circularly polarized light available at 0.3 mrad below the positron orbit plane, with a rate of about 70%.<sup>18</sup> ID12A provides circularly polarized radiation generated by a helical undulator (Helios II). Here, the polarization rate after the cryogenically cooled Si(111) double crystal monochromator is near 95% at the Gd  $L_{2,3}$  edges.<sup>19</sup> The spectra were recorded either in transmission mode (D11) or in the total fluorescence-yield (TFY) mode (ID12A).

The XA spectra in the soft x-ray range [ $M_{4,5}(3d \rightarrow 4f)$  edges of Gd] were measured in transmission mode (on the lattice-expanded GdN layers) at the beamline SU22 of the Super-ACO storage ring at LURE.<sup>20</sup> It supplies a monochromatic beam by a double-crystal monochromator and is equipped with an UHV system. An asymmetric wiggler provides light with a circular polarization rate near 30% (SU22) in the energy ranges of interest. As the spectra were measured in transmission mode it was important to chose weakly absorbing substrates (here Mylar foil, 1.5  $\mu\text{m}$  thick) and to keep the layers sufficiently thin in order to have about 50% of transmission.

XMCD experiments probe the absorption cross section at a core-level threshold of a material with a net magnetic moment for two opposite relative orientations of the magnetization and helicity of circularly polarized photons. The difference of the spectra probes the net magnetic moment through transfer of the x-ray angular momentum vector in the absorption process. In our study, the XMCD spectra of the GdN layers were recorded across a given absorption edge at constant beam helicity for two opposite directions of the magnetization at saturation induced by applying a magnetic field parallel and opposite to the x-ray propagation direction at grazing incidence [20 kOe at 30° (D11 and SU22), 30 kOe at 10° (ID12A)]. At beamlines SU22 and ID12A the field was inverted at each energy point. The energy-dispersive setup of D11 permits simultaneous data acquisition at all energies in a chosen interval; here, the magnetic field was inverted between two successive spectra. Good statistics were obtained

by recording a large number of spectra. For the absorption measured in transmission mode (D11, SU22), if  $\mu^-(H_{+,-})$  and  $\mu^+(H_{+,-})$  represent the normalized absorption coefficients for right- and left-circularly polarized photons (helicity  $-\hbar$ ,  $+\hbar$ , respectively) and for the two magnetic-field directions  $H_+$  parallel and  $H_-$  antiparallel to the propagation direction of the light, the XMCD signal is defined as  $\mu^-(H_+) - \mu^-(H_-)$  or  $\mu^+(H_-) - \mu^+(H_+)$  for the two helicities, respectively. In case of the absorption measured in the TFY mode (D12A), the XMCD signal is simply given by the difference between the normalized absorption signals  $I^+$  and  $I^-$  for the two field directions  $H_+$  and  $H_-$  at photon helicity  $-\hbar$ . These definitions correspond to the generally accepted convention. All spectra presented were corrected for 100% circular polarization. The TFY spectra were corrected for saturation effects,<sup>21</sup> which are small in the present case.

### III. X-RAY-ABSORPTION SPECTROSCOPY: RESULTS AND DISCUSSION

Ferromagnetism of GdN is dominated by the interacting large spin magnetic moments of the  $4f$  electrons. Local access to the  $4f$  states is provided by measurements of XA and XMCD at the  $M_{4,5}$  absorption edges of Gd probing the  $3d \rightarrow 4f$  resonant transition. Such spectra recorded below  $T_C$  on the layers deposited at room temperature (lattice-expanded layers) show the general shape and structure characteristic<sup>22</sup> of  $\text{Gd}^{3+}$ . The spontaneous  $4f$  spin moment derived from the low-temperature XMCD spectra by means of the sum rules<sup>23</sup> is consistent with the Hund's rule value of this ion; as expected, there is no  $4f$  orbital moment. These observations agree with the previous ones made on the bulklike layers deposited at 450 °C.<sup>10</sup> Hence the spectra are not reproduced here. Moreover, the integrated dichroic signal shows the same temperature dependence as the macroscopic magnetization of the layers in both cases, i.e., the local magnetization of the Gd- $4f$  orbitals follows that of the entire layers. The only difference is reflected in the reduced Curie temperature  $T_C$  of the lattice-expanded layers, which is near 30 K as was already indicated (Sec. II A). This will be further addressed below.

Calculations of the electronic band structure of GdN reveal a fundamental involvement of the Gd- $5d$  electronic band states in the formation of magnetic order in GdN.<sup>7-9,24</sup> In the ground state of GdN, the Gd- $5d$  states, split into states of  $t_{2g}$  and  $e_g$  symmetry in the cubic crystal field (with the  $e_g$  states at energies above the  $t_{2g}$  states), feel the exchange field created by the  $4f$  electrons and are spin split, as are the N- $2p$  states. The splitting of the majority- and minority-spin bands strongly depends on momentum and energy of the band states. The majority Gd- $5dt_{2g}$  band is expected to overlap the majority N- $2p$  band at  $E_F$ , forming a N- $p$ -derived hole pocket at the  $\Gamma$  point and a predominantly Gd- $5dt_{2g}$ -derived electron pocket at the  $X$  point of the Brillouin zone; there is an indirect gap in the respective minority bands, hence half metallicity, with a small contribution to the overall spontaneous magnetic moment of the ferromagnet though.<sup>7,11</sup> The density states at  $E_F$  is low and the states are slightly occupied.<sup>7</sup> Upon volume expansion, which is relevant for the present study, the Gd- $5d$  bands move up rela-

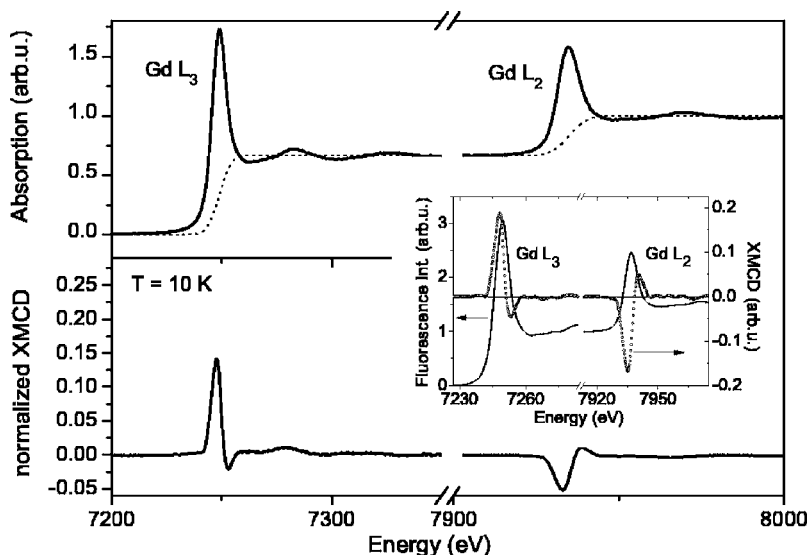


FIG. 1. X-ray absorption and XMCD spectra at the  $L_3$  and  $L_2$  edges of Gd for a lattice-expanded GdN layer deposited on a Kapton substrate at room temperature (main figure, measured in transmission mode) and a bulklike GdN layer deposited on a Si substrate at 450 °C (inset, measured in total fluorescence yield mode). GdN layer thickness 2000 Å. Measurements at 10 K. The step heights at the absorption edges are normalized to a ratio of 2 to 1, using arctan step functions, in order to take into account the degeneracy of the  $2p_{3/2}$  and  $2p_{1/2}$  core states (see dotted line in the main figure).

tive to the N-2p bands, decreasing the occupation of the  $5d_{2g}$  states near the X point.<sup>8,13</sup> XA and XMCD spectra at the Gd- $L_{2,3}$  absorption edges, essentially involving the  $2p \rightarrow 5d$  electric dipole transitions, probe the  $5d$  character of the unoccupied low-lying conduction-band states at the Gd sites and their magnetic polarization. Figure 1 displays such spectra of a lattice-expanded GdN layer measured at 10 K in transmission mode. They are essentially identical in shape with the Gd  $L_{2,3}$ -edge spectra measured on a bulklike GdN layer in total fluorescence yield mode (Fig. 1, inset). The presence of magnetic dichroism demonstrates that the Gd- $5d$  states indeed carry an ordered magnetic moment. The isotropic  $L_2$  and  $L_3$  XA spectra in Figs. 1 exhibit a pronounced singularity at the threshold (“white line”) which is broadened due to the finite lifetime of the  $2p$  core hole. It is superposed on a steplike increase of the absorption due to the transitions into the continuum states. Two arctan step functions were used (dotted lines in Fig. 1) to normalize the spectra to a jump ratio of 2:1 at the  $L_3$  and  $L_2$  edges which reflects the statistical branching ratio according to the degeneracy of the  $2p$  core states. The  $L_2$  and  $L_3$  XMCD spectra in Fig. 1, opposite in sign, show the line shape documented in the literature for metallic<sup>25,26</sup> or insulating<sup>27,28</sup> Gd-based compounds, which are quite similar. They are characterized by an intense peak on the low-energy side preceding a small tail of opposite sign on the high-energy side. The most intense part is observed at somewhat lower energy than the maximum of the isotropic XA signal. The predominant sign of the dichroic signals [positive at the  $L_3$  edge and negative at the  $L_2$  edge for the present conventional definition (Sec. II B)] agrees with that observed for Gd metal<sup>29</sup> and insulating  $\text{Gd}_3\text{Ga}_5\text{O}_{12}$ ,<sup>27</sup> for example. It shows that, as in these solids, the ordered Gd- $5d$  magnetic moment is aligned parallel to the  $4f$  moment pointing along the direction of the magnetic field applied in the measurement. This alignment is expected for GdN from the electronic-structure calculations.<sup>7,9,24</sup>

Let us note that the relation between the orientation of the Gd- $5d$  magnetic moment and the sign of the corresponding XMCD signal is opposite to what is expected in a simple

single-particle description<sup>29,30</sup> of circular magnetic dichroism in XA. In fact, dichroism in the  $2p$ -to- $5d$  transition in the RE does not simply result from the difference in occupation of spin-split  $5d$ -derived conduction bands in the ground state, i.e., from the  $5d$ -electron magnetic polarization. A rigorous description of the absorption process must consider the dynamics of the excitation and the matrix element for the transition between the initial and each final state. All modifications of the wave function that are caused by the excitation will contribute to the matrix element. In this context, Harmon and Freeman have shown that the strong intra-atomic  $4f$ - $5d$  exchange interaction in the RE makes the radial part of the  $2p$ - $5d$  dipole matrix element dependent on the relative spin orientation of the  $4f$  and photoexcited  $5d$  electrons, resulting in a higher value in the parallel case.<sup>25,31–33</sup> They concluded that the combination of band-structure effects and intra-atomic final state interaction in the absorption process may reverse the sign of the dichroic spectra as it is always observed in the case of the Gd- $L_{2,3}$  edges, here for the present compound. Baudelet *et al.*<sup>14</sup> were the first to recognize by systematic experimentation that the  $4f$ - $5d$  exchange interaction is effective in the photoabsorption process at the  $L_{2,3}$  resonances of all RE and makes it very complex. As a result, the sum rules that relate the integrated XMCD intensities to the expectation value of the ordered spin and orbital magnetic moments in the ground state<sup>23</sup>—and are a powerful tool regarding the less complex  $3d$  transition-metal  $L_{2,3}$  edges—are not applicable in the case of the RE  $L_{2,3}$  edges. In particular, no definite conclusion can be drawn on the eventual presence of a Gd- $5d$  orbital magnetic moment in GdN that might be involved, via Gd- $5d$ -N- $2p$  hybridization, in generating the orbital-moment derived XMCD signal observed at the N- $K$  edge, as hypothesized before.<sup>10</sup> Generally, model calculations<sup>15–17</sup> of the RE  $L_{2,3}$  spectra have provided basic insights. They were successful, for example, in describing basic trends in the sign and the widely varying ratios of the dichroic signals in RE-based metallic compounds previously investigated.<sup>14</sup> Nevertheless, theoretical understanding of the spectra remains rather limited to date.

The amplitudes of the Gd- $L_2$  and  $L_3$ -edge XMCD signals decrease with increasing temperature in the same way as the

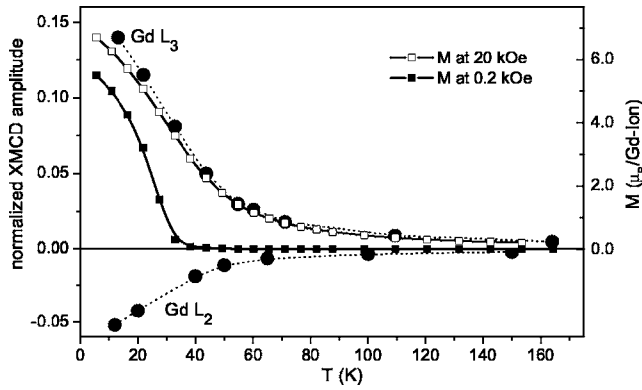


FIG. 2. Normalized XMCD amplitudes at the Gd- $L_2$  and - $L_3$  absorption edges of a lattice-expanded GdN layer (2000 Å) as a function of temperature  $T$  (full circles). The temperature dependence of the  $L_3$ -edge XMCD signal is compared with that of the macroscopic magnetization  $M$ , measured in the same magnetic field (open squares). Full squares: temperature variation of the low-field (200 Oe) magnetization  $M$ .

macroscopic long-range magnetization of the GdN layers, a correlation equally observed for the Gd-4*f* magnetic moment. In Fig. 2 this correspondence is illustrated for the  $L_3$ -edge signal, measured in a magnetic field of 20 kOe as the magnetization, in the magnetically saturated state. The thermal variation of the low-field (200 Oe) global magnetization shown for comparison indicates a reduction of the Curie temperature of the volume-expanded GdN layer: we have  $T_C \approx 30$  K as compared to value of  $\sim 60$  K observed<sup>10</sup> for the bulklike layers. Raising the applied field to 20 kOe broadens the transition. Note that the dichroic signal remains finite at 150 K. The reduction of  $T_C$ , which reflects a significant modification of the exchange interactions, is the most distinct effect visible on the macroscopic magnetic properties that results from an increase of the lattice parameter of the GdN layers. Basic insight into the underlying mechanism can be obtained from a simple mean-field model applied to fcc GdN. Assuming exchange interactions between the nearest and next-nearest Gd-neighbor 4*f* magnetic moments given by the parameters  $J_1$  and  $J_2$ , respectively, we have

$$K_B T_C \alpha 12J_1 + 6J_2. \quad (1)$$

Symmetry considerations suggest nearest-neighbor (NN) exchange  $J_1$  in GdN to be mediated essentially by the Gd-5*dt*<sub>2g</sub> orbitals (directed to the next cation), next-nearest-neighbor (NNN) exchange  $J_2$  by the Gd-5*de*<sub>g</sub> orbitals (directed to the anion) via the anion *p* orbitals.<sup>34</sup> Existing calculations of the exchange parameters, even though based on quite different theoretical approaches, agree in that the two terms in Eq. (1) compete:  $J_1$  represents ferromagnetic (FM) and  $J_2$  antiferromagnetic (AFM) coupling,<sup>11,35</sup> where  $J_1$  prevails, i.e.,  $|J_1| \gg |J_2|$ . Furthermore, the exchange parameters depend strongly on the lattice constant: FM  $|J_1|$  decreases and AFM  $|J_2|$  is strengthened with increasing lattice constant  $a$ , both with a similar slope  $\delta|J_{1,2}|/\delta a$ .<sup>11</sup> Then, according to Eq. (1), expanding the GdN lattice (by layer deposition at room temperature) implies a reduction of the Curie tempera-

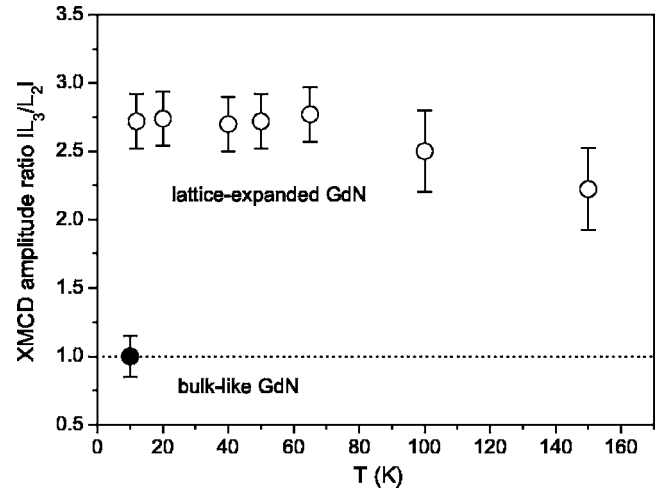


FIG. 3. Ratio of the Gd  $L$ -edge XMCD amplitudes,  $|L_3/L_2|$ , at different temperatures for a lattice-expanded (open circles) and bulklike (full circle) GdN layer (2000 Å). Straight dotted line: the value 1 is expected from the degeneracy of the  $2p_{1/2}$  and  $2p_{3/2}$  core states.

ture  $T_C$ , essentially by weakening of FM exchange coupling; AFM exchange gains in importance, even though this effect is small in view of its low absolute value.

A remarkable observation made on the volume-expanded GdN layers, but not on the bulklike one, is the unusual ratio of the Gd  $L$ -edge XMCD amplitudes,  $|L_3/L_2|$ , which amounts to almost 3 up to  $\sim 100$  K and then decreases slightly toward higher temperature (Fig. 3). The values observed are far above the statistical value of 1 imposed by the degeneracy of the  $2p_{1/2}$  and  $2p_{3/2}$  core states. The statistical value, to our knowledge, so far has been always observed for Gd-based systems (see, e.g., Ref. 14), in agreement with existing model calculations;<sup>15–17</sup> it can be seen in Fig. 3 (and directly in the inset in Fig. 1) that it is also found for the bulklike GdN layer, which behaves quite “normal.” The present result for the lattice-expanded GdN layers adds further complexity to the understanding of the RE  $L_{2,3}$ -edge XMCD spectra. It is an important observation that the enhanced  $|L_3/L_2|$  XMCD ratio in the volume-expanded GdN layers is essentially the result of a reduced amplitude of the  $L_2$ -edge dichroic signal, since the  $L_3$ -edge XMCD amplitude differs much less from that of the bulklike layer (Fig. 1). Unfortunately, the theoretical understanding of the RE  $L_{2,3}$ -edge XMCD spectra is very limited. It is not obvious why the dichroic  $L_{2,3}$ -edge amplitudes respond differently to an enlargement of the lattice constant of the GdN layers. From a naive viewpoint, a reduced XMCD amplitude might be attributed to a diminished spin polarization, i.e., to a change of the relative occupation of the low-lying unoccupied majority- and minority-spin conduction bands, and/or to modified transition probabilities to these bands in the absorption process. Changes in the relative occupation of the spin-up and spin-down 5*d*-derived bands upon lattice expansion might occur due to their shift relative to  $E_F$ <sup>11,13</sup> and/or to a reduced (energy dependent) exchange splitting, for example. Such effects concern the low-lying conduction-band states in particular, which are essentially Gd-5*dt*<sub>2g</sub> derived

and of majority-spin character.<sup>7-9,24</sup> It may not be entirely unexpected then that especially the  $L_2$ -edge XMCD spectra are affected by an expansion of the GdN lattice. This is because different final states are probed at the  $L_2$  and  $L_3$  thresholds, i.e., the states Gd- $5d_{3/2}$  and  $5d_{5/2}$ , respectively, and the  $5dt_{2g}$  states have a stronger  $j=3/2$  character compared to the  $5de_g$  states, which have a stronger  $j=5/2$  character.<sup>36</sup> We note that we have observed this preferred relation between the dichroic  $L_2$ - and  $L_3$ -edge signals and the  $5dt_{2g}$  and  $5de_g$  states, respectively, already previously upon hydrogen charging of RE-based multilayers.<sup>37</sup> Here, to pursue this line of reasoning, the reduction of  $T_C$ , essentially due to a diminished FM NN exchange parameter involving the  $5dt_{2g}$  states (as we have argued above), lends further support to this argument.

The particular role of the Gd- $5dt_{2g}$  states for ferromagnetic order in GdN, reflected in the response of  $T_C$  and in the different sensitivity of the Gd- $L_2$  and  $L_3$  XMCD spectra to a lattice expansion of the layers, is also observed in the isotropic  $L_2$  XA spectrum probing the  $5d_{3/2}$  states. Upon entering the ferromagnetic phase the Gd- $5d$  states experience spin splitting by the exchange interaction with the  $4f$  electron spins. As a result, the majority-spin  $5d$ -derived conduction bands are pushed to lower energies such that the indirect band gap is expected to close for this spin channel, i.e., the majority Gd- $5dt_{2g}$  band at  $\Gamma$  overlaps the N- $2p$  band at  $E_F$ ,<sup>7,9,11,24</sup> a lowering of  $\sim 0.3$  eV of the optical absorption onset at  $T \ll T_C$  has been predicted as a consequence.<sup>24</sup> We have found (Fig. 4) that the effect leads to (i) a reduced white line at the Gd- $L_2$  XA edge, which indicates a decrease of the density of unoccupied  $5d$ -derived states probed, and (ii) a measurable “redshift” of the edge, amounting to a maximum of  $\sim 0.5$  eV at 12 K. There is strong evidence that the edge shift is a signature of ferromagnetic ordering in GdN, since it follows the amplitude of the  $L_2$ -edge XMCD signal down to low temperatures that varies as the long-range magnetization [Fig. 4(b)]. That is, the shift is proportional to the exchange splitting of the Gd- $5d$ -derived conduction band. We note that a similar effect was observed on EuO, a compound with many comparable electronic characteristics as GdN: a shift to lower energies of the XA onset at the O-K( $1s$ ) edge occurs upon entering the ferromagnetic state.<sup>38</sup> Interestingly, for GdN the effect is essentially restricted to the Gd- $L_2$  edge, as can be seen in Fig. 4: a shift of the  $L_3$  XA threshold, if occurring at all, would be at most 0.1 eV, our estimate of the statistical error. This again emphasizes the different involvement of the Gd- $5dt_{2g}$  and  $-5de_g$  conduction-band states in the ferromagnetic phase transition.<sup>39</sup>

#### IV. CONCLUSION

Films of the ferromagnet GdN deposited at room temperature show a nearly 9% larger unit-cell volume than films deposited at elevated temperature with a lattice parameter close to that of the bulk compound. While the good stoichiometry is preserved upon lattice expansion the Curie temperature  $T_C$  is significantly reduced in the nonequilibrium situation, indicating a reduced exchange interaction responsible for FM order. Measurements of XMCD spectra at the Gd- $L_{2,3}$  ( $2p \rightarrow 5d$ ) absorption edges, carried out to probe the

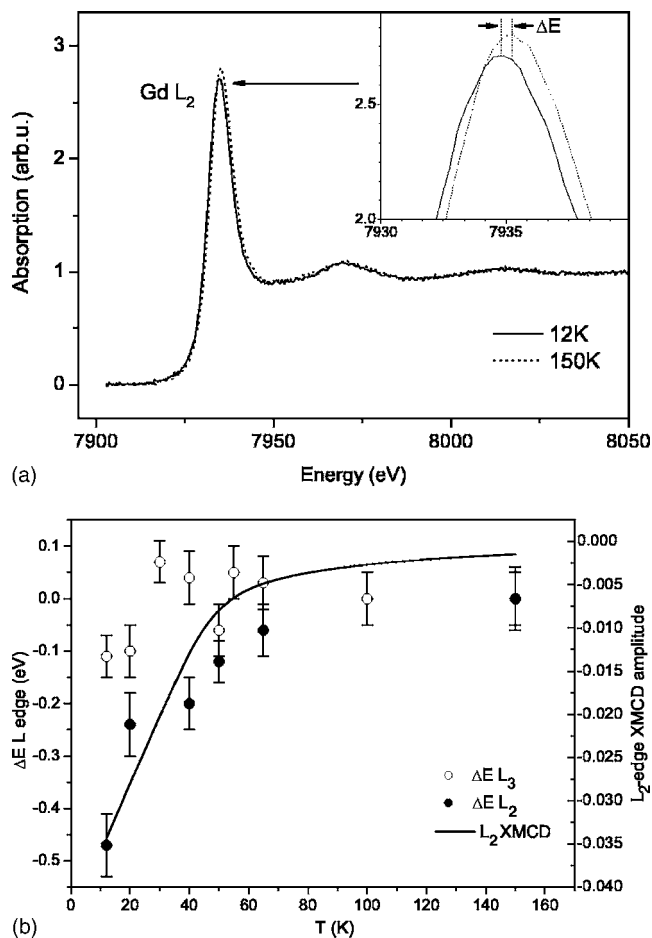


FIG. 4. For a GdN layer (2000 Å) deposited at room temperature: (a) x-ray-absorption spectra at the Gd- $L_2$  edge at 12 and 150 K. Insert: enlarged view around the peak. (b) deviation  $\Delta E$  of the  $L_2$  and  $L_3$  XA peak locations from the value at 150 K, derived by deconvolution of the measured XA spectra with a Lorentzian function and an arctan step function. Solid line: temperature variation of the  $L_2$ -edge XMCD amplitude.

$4f$ -induced magnetic polarization of the Gd- $5d$ -derived conduction-band states, lead to an intricate observation: the ratio of the amplitudes of the dichroic signals,  $|L_3/L_2|$ , of the volume-expanded layers is up to three times higher, essentially due to a reduced  $L_2$  XMCD signal, than the statistical value imposed by the degeneracy of the  $2p$  core states, which is observed for the bulklike layers. A clear-cut explanation is not possible at this stage, since theoretical understanding of the complex  $L$ -edge spectra of the RE in XA is very limited. However, we suggest that some basic insight can be gained by considering that different Gd- $5d$ -derived final states are probed in the absorption process at the  $L_2$  and  $L_3$  thresholds which play a different role in mediating magnetic order of the  $4f$  electrons. Existing calculations of the electronic band structure of GdN highlight that essentially the Gd- $5dt_{2g}$  states are involved, which form the bottom of the conduction band and experience exchange splitting below  $T_C$ . We have found that this splitting leads to a measurable shift of the  $L_2$  absorption edge to lower energies, while the  $L_3$  edge position stays inert. We attribute this difference to the strong  $j=3/2$  character of the  $5dt_{2g}$  states, which relates them essentially to

the  $L_2$ -edge absorption. In contrast, the  $L_3$ -edge absorption mainly probes the  $5de_g$  states due to their stronger  $j=5/2$  character. We argue that the shift in energy of the  $L_2$  absorption edge upon ferromagnetic ordering and the reduction of  $T_C$  and of the XMCD  $L_2$ -edge amplitude are essentially related to a modification of the  $5dt_{2g}$ -derived conduction band upon lattice expansion of the layers.

## ACKNOWLEDGMENTS

Enlightening discussions with G. Krill (Orsay) and K. Samwer (Göttingen) are gratefully acknowledged. We thank the beamline staffs at LURE and the ESRF for technical support. This work was supported by the Deutsche Forschungsgemeinschaft within SFB 602.

\*Author to whom correspondence should be addressed. Electronic address: wfelsch@gwdg.de

- <sup>1</sup>T. R. McGuire, R. J. Gambino, S. J. Pickart, and H. A. Alperin, *J. Appl. Phys.* **40**, 1009 (1969).
- <sup>2</sup>R. J. Gambino, T. R. McGuire, H. A. Alperin, and S. J. Pickart, *J. Appl. Phys.* **41**, 933 (1970).
- <sup>3</sup>W. Stutius, *Phys. Kondens. Mater.* **10**, 152 (1969).
- <sup>4</sup>P. Wachter and E. Kaldis, *Solid State Commun.* **34**, 241 (1980).
- <sup>5</sup>R. A. Cutler and A. W. Lawson, *J. Appl. Phys.* **46**, 2739 (1975).
- <sup>6</sup>D. X. Li, Y. Haga, H. Shida, T. Suzuki, Y. S. Kwon, and G. Kido, *J. Phys.: Condens. Matter* **9**, 10777 (1997).
- <sup>7</sup>C. M. Aerts, P. Strange, M. Horne, W. H. Temmerman, Z. Szotek, and A. Svane, *Phys. Rev. B* **69**, 045115 (2004).
- <sup>8</sup>A. Hasegawa and A. Yanase, *J. Phys. Soc. Jpn.* **42**, 492 (1977).
- <sup>9</sup>A. G. Petukhov, W. R. L. Lambrecht, and B. Segall, *Phys. Rev. B* **53**, 4324 (1996).
- <sup>10</sup>F. Leuenberger, A. Parge, W. Felsch, K. Fauth, and M. Hessler, *Phys. Rev. B* **72**, 014427 (2005).
- <sup>11</sup>C. Duan, R. F. Sabiryanov, J. Liu, and W. N. Mei, *Phys. Rev. Lett.* **94**, 237201 (2005).
- <sup>12</sup>M. Horne, P. Strange, W. M. Temmermann, Z. Szotek, A. Svane, and H. Winter, *J. Phys.: Condens. Matter* **16**, 5061 (2004).
- <sup>13</sup>M. D. Johannes and W. E. Pickett, cond-mat/0508241 (unpublished).
- <sup>14</sup>F. Baudelet, C. Giorgetti, S. Pizzini, C. Brouder, E. Dartyge, A. Fontaine, J. P. Kappler, and G. Krill, *J. Electron Spectrosc. Relat. Phenom.* **62**, 153 (1993).
- <sup>15</sup>T. Jo and S. Imada, *J. Phys. Soc. Jpn.* **62**, 3721 (1993).
- <sup>16</sup>H. Matsuyama, I. Harada, and A. Kotani, *J. Phys. Soc. Jpn.* **66**, 337 (1997); H. Matsuyama, K. Fukui, H. Maruyama, I. Harada, and A. Kotani, *J. Magn. Magn. Mater.* **177-181**, 1029 (1998); H. Matsuyama, K. Fukui, K. Okada, I. Harada, and A. Kotani, *J. Electron Spectrosc. Relat. Phenom.* **92**, 31 (1998).
- <sup>17</sup>M. van Veenendaal, J. B. Goedkoop, and B. T. Thole, *Phys. Rev. Lett.* **78**, 1162 (1997); *J. Electron Spectrosc. Relat. Phenom.* **86**, 151 (1997).
- <sup>18</sup>F. Baudelet, E. Dartyge, A. Fontaine, C. Brouder, G. Krill, J.-P. Kappler, and M. Piecuch, *Phys. Rev. B* **43**, 5857 (1991).
- <sup>19</sup>J. Goulon, A. Rogalev, C. Gautier, C. Goulon-Ginet, S. Paste, R. Signorato, C. Neumann, L. Varga, and C. Malgrange, *J. Synchrotron Radiat.* **5**, 232 (1998).
- <sup>20</sup>P. Sainctavit, D. Lefèbvre, M.-A. Arriot, C. Cartier dit Moulin, J. P. Kappler, J. P. Schillè, G. Krill, C. Brouder, and M. Verdager, *Jpn. J. Appl. Phys., Part 1* **32**, 295 (1992); D. Lefèbvre, Ph. Sainctavit, and C. Malgrange, *Rev. Sci. Instrum.* **65**, 2556 (1994).
- <sup>21</sup>S. Eisebitt, T. Böske, J.-E. Rubensson, and W. Eberhardt, *Phys. Rev. B* **47**, 14103 (1993).

- <sup>22</sup>B. T. Thole, G. van der Laan, J. C. Fuggle, G. A. Sawatzky, R. C. Karnatak, and J.-M. Esteve, *Phys. Rev. B* **32**, 5107 (1985); J. B. Goedkoop, B. T. Thole, G. van der Laan, G. A. Sawatzky, F. M. F. de Groot, and J. C. Fuggle, *ibid.* **37**, 2086 (1988).
- <sup>23</sup>B. T. Thole, P. Carra, F. Sette, and G. van der Laan, *Phys. Rev. Lett.* **68**, 1943 (1992); P. Carra, B. T. Thole, M. Altarelli, and X. Wang, *ibid.* **70**, 694 (1993); M. Altarelli, *Phys. Rev. B* **47**, 597 (1993).
- <sup>24</sup>W. R. L. Lambrecht, *Phys. Rev. B* **62**, 13538 (2000).
- <sup>25</sup>J. C. Lang, X. Wang, V. P. Antropov, B. N. Harmon, A. I. Goldman, H. Wan, G. C. Hadjipanayis, and K. D. Finkelstein, *Phys. Rev. B* **49**, 5993 (1994).
- <sup>26</sup>R. M. Galera, S. Pizzini, J. A. Blanco, J. P. Rueff, A. Fontaine, Ch. Giorgetti, F. Baudelet, E. Dartyge, and M. F. López, *Phys. Rev. B* **51**, 15957 (1995).
- <sup>27</sup>J. B. Goedkoop, A. Rogalev, M. Rogaleva, C. Neumann, J. Goulon, M. van Veenendaal, and B. T. Thole, *J. Phys. IV* **7**, C2-415 (1997).
- <sup>28</sup>C. Neumann, B. W. Hoogenboom, A. Rogalev, and J. B. Goedkoop, *Solid State Commun.* **110**, 375 (1999).
- <sup>29</sup>G. Schütz, M. Knülle, R. Wienke, W. Wilhelm, W. Wagner, P. Kienle, and R. Frahm, *Z. Phys. B: Condens. Matter* **73**, 67 (1988).
- <sup>30</sup>P. Carra and M. Altarelli, *Phys. Rev. Lett.* **64**, 1286 (1990); P. Carra, B. N. Harmon, B. T. Thole, M. Altarelli, and G. A. Sawatzky, *ibid.* **66**, 2495 (1991).
- <sup>31</sup>B. N. Harmon and A. Freeman, *Phys. Rev. B* **10**, 1979 (1974).
- <sup>32</sup>X. Wang, T. C. Leung, B. N. Harmon, and P. Carra, *Phys. Rev. B* **47**, 9087 (1993).
- <sup>33</sup>J. C. Lang, S. W. Kycia, X. D. Wang, B. N. Harmon, A. I. Goldman, D. J. Branagan, R. W. McCallum, and K. D. Finkelstein, *Phys. Rev. B* **46**, 5298 (1992).
- <sup>34</sup>S. Methfessel, *Z. Angew. Phys.* **18**, 414 (1965).
- <sup>35</sup>T. Kasuya and D. X. Li, *J. Magn. Magn. Mater.* **167**, L1 (1997); *Physica B* **230-232**, 472 (1997).
- <sup>36</sup>M. Imada, A. Fujimori, and Y. Tokura, *Rev. Mod. Phys.* **70**, 1040 (1998).
- <sup>37</sup>M. Münzenberg, F. Leuenberger, W. Felsch, G. Krill, T. Neisius, S. Pascarelli, and S. Pizzini, *Phys. Rev. B* **67**, 224431 (2003).
- <sup>38</sup>P. G. Steeneken, Ph.D. thesis, University of Groningen, Groningen, 2002, Chap. 5; <http://www.ub.rug.nl/eldoc/dis/science/p.g.steeneken/>
- <sup>39</sup>The shift of the  $L_2$  XA onset was only measured here on a lattice-expanded GdN layer. However, we do not attribute it to a structural effect. Its existence for the bulklike layer is reasonable to assume.